Chapter 16
Solar-Electric Long Endurance Reflector Craft for Meteorology and Climate Simulation

Narayanan M. Komerath, Ravi Deepak, and Adarsh Deepak

Nomenclature

AR	Aspect Ratio
CO2	Carbon dioxide
FL	Flying Leaf. Large-span, infinite endurance ultralight reflector vehicle
FLT	Carrier vehicle to take FL sheets to high altitude
GB	Glitter Belt architecture of mesospheric reflectors
HALE	High Altitude Long Endurance (aircraft)
ISA	International Standard Atmosphere.
MSL	Altitude above Mean Sea Level standard day, ISA
W/S	Wing Loading. Ratio of vehicle weight to lifting surface planform area.

16.1 Introduction

Today's efforts to combat climate change have focused on reducing infrared-absorbing CO_2 and other greenhouse gases. Meanwhile, thermodynamic heat engine efficiency of industrial economies has gone down, with 67% of heat input being released into the atmosphere as waste heat (Smil 2021). Scientists and political leaders are increasingly agreeing that some form of direct intervention will be necessary to buy time for other measures to take effect. One intervention is to reduce the amount of solar radiation (insolation) reaching the lower atmosphere. The Glitter Belt architecture, discussed in prior work (Komerath et al. 2021a, b), meets

N. M. Komerath (✉) · R. Deepak · A. Deepak
Taksha Institute, Silicon Valley, CA, USA

Taksha Institute, Hampton, VA, USA

T. H. Karakoc et al. (eds.), *Advances in Electric Aviation*, Sustainable Aviation,
https://doi.org/10.1007/978-3-031-32639-4_16

all criteria set out by the US National Academy of Sciences for sunlight-reflecting projects. At the outset, the vehicles described here serve as meteorological platforms ale to loiter over the most remote areas of the planets such as the southern oceans. They thus complement space satellites move at over 400 km altitude and 25,000 kmph, challenging resolution and persistence. Aircraft carry radiosondes and other instruments, with special missions using expendable drop-sondes for vertical profile data of the atmosphere. The Flying Leaflets described below offer unprecedented coverage, persistence, and resolution over remote areas.

16.1.1 Prior Work: FL and FLT

The Glitter Belt architecture (Komerath et al. 2017) will place swarms of ultralight reflector vehicles at 30.5 km altitude. Initially, these will be concentrated where summer is at its peak. The chosen altitude is high enough that solar intensity is at the full value seen in space at Earth's orbit around the Sun. The Glitter Belt architecture is conceived and built from just two types of vehicles. One is the Flying Leaflet, sized for takeoff from small fields (Fig. 16.1 (left)), a solar-powered flying wing carrying a rolled-up sheet of reflective Mylar and a framework to support the sheet. This vehicle ascends to 30.5 km inside 8 hours, but cannot survive night-time glide without coming below the 18.3 km limit of Class A airspace. The second type of vehicle is the Flying Leaf (FL) in Fig. 16.1 (right), assembled at high altitude by in-flight wing-tip rendezvous and attachment of 11 Flying Leaflets (FLTs). The FLT is a 32 m-span, 4 m-chord flying wing with 4 BLDC motor-driven propellers, carrying a deployable Mylar sheet. It has a solar panel area set at 40% of its wing area, including over the leading and trailing edges and upper surface. The solar panels are assumed to be of 20% efficiency.

The Way to 30.5 km Altitude

A mission profile is shown in Fig. 16.2. FLTs takeoff on a summer morning, climbing to 30.5 km by 4 pm. They join with 10 other FLTs, with 8 of 11 returning, leaving their sheets and sheet-frames attached to the FL. The FLs form into swarms for

Fig. 16.1 1 (Left) 32 m × 4 m, 4-propeller FLT with partially deployed sheet above. (Right) 353 m × 32 m FL

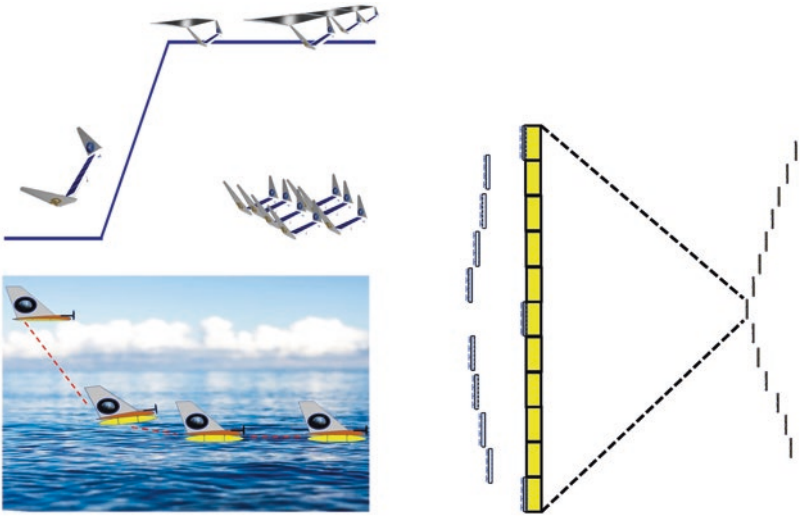

Fig. 16.2 FLT mission profile. (With permission)

Fig. 16.3 Prior HALE vehicles: The NASA Pathfinder, Helios 1, and Helios 3. From Ravikovich et al. (2021) and Wikipedia

easier control and for distributed antenna functions. Solar power rises with altitude, from about 1.0 to 1.367 kW/m^2. Temperature varies from 85 °C when exposed to the sun, to below −57 °C at night in the stratosphere. Strongest winds are in the lower stratosphere during initial climb; while dynamic pressure is highest close to sea level. Motor cooling in solar-heated, near-vacuum, rendezvous and swarm operation for high-precision distributed antenna applications pose challenges.

16.2 Conceptual Design

Figure 16.3 shows three successful HALE concepts: The NASA Pathfinder, Helios-1, and Helios-2 used to benchmark the FLT and FL concepts. Relevant parameters are shown in Table 16.1. Our FLT and FL aspire to far lower wing loading (W/S) than prior concepts. This is because much of the lift is carried by the large area of ultrathin reflective sheets, supported by a carbon fiber truss and grid.

Table 16.1 Benchmarking

	Pathfinder	Pathfinder +	Centurion	Helios HP01	Helios HP03	FLT 32 m	FL 32 × 11	FL64 × 11
Length	3.6	3.6	3.6	3.6	5	6	6	6
MAC	2.4	2.4	2.4	2.4	2.4	4	32	64
Span m	29.5	36.3	61.8	75.3	75.3	32	352	704
W/S N/m^2	34.9	35.4	57.0	50.4	57.0	10.4	1.2	1.2
AR	12.3	15.1	25.8	31.4	31.4	8.0	11.0	11.0
MTOW, kg	252	315	862	929	1052	135	1379	5517
Payload, kg	45	67.5	270	329		50	150	300
Hmax. Fl, m	21,802	24,445		29,523	19,812	35,661	35,661	35,661
Motor: BLDC1.5 kW	1.50	1.50	1.50	1.50	1.50	1.5	1.5	1.5
# of motors	6	8	14	14	10	4	12	12
Nsum, KW	12	16	28	28	20	6	18	18
Max pover SC, kW	8	13	31	35	18.5			
Add'l battery	NiCd		NiCd	LiPO	LiPO, airH2	LiPo	LiPo	LiPo

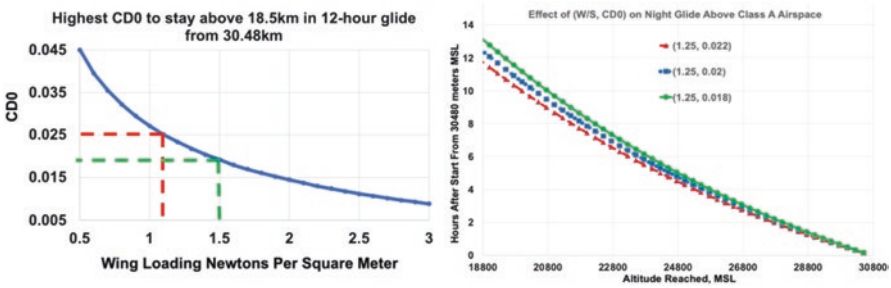

Fig. 16.4 (Left) Highest value of profile drag coefficient at each wing loading, to stay up above 18.3 km in 12-h glide. (Right) Effect of profile drag coefficient on glide timeline, at W/S of 1.25 Pascals. From Komerath et al. (2021b), with permission

Figure 16.4 (left) shows necessary performance parameters to stay above Class A airspace. The zone between red and green vertical dashed lines is feasible, with CD0 below 0.025, and wing loading below 1.5 Pascals. Figure 16.4 (right) shows how descent profile varies with profile drag coefficients. The notion of joining wings at the tip to increase aspect ratio, decrease induced drag coefficient, and increase range, has been discussed in Quinlan (2019). Wu et al. (2021) have explored joining 2–6 single-propeller wing-tail UAVs at the wingtips. We note in passing that with sufficient control to perform rendezvous, it is also possible to form swarms of sufficient precision to act as synthetic aperture antennae.

Very large antennae can be formed with FLs, a topic for future discussion. In the FL, the main power source is solar panels (assumed 20% efficient) (Ackermann

et al. 2021; Kleemann et al. 2020) covering 40–85% of the FLT wings including around the leading edge to capture low-horizon sunlight, and some on the bottom surface to pick up diffused cloud reflections. A small battery (100 Wh) is provided to operate instruments and communications. A generator charges the batteries. Propeller windmilling can recover some power, keeping the battery charged, and enabling a burst flare maneuver for landing at night. The lift and drag coefficient data for a thin cambered flat plate were used to model the lifting sheet (Gilbert 2020). Maximum lift coefficient is 1.2. We restrict operations to CL of 1.0. Structural weight was modelled assuming the technology of the benchmark vehicles of Fig. 16.3 to estimate the total weight of the FLTs and known strength/weight profile of carbon fiber beams supporting the thin (0.05 kg/m^2) aluminized Mylar sheets. Figure 16.5 shows that FLT models smaller than 30 m span may not be able to stay above 18.3 km through the night.

Space limitations prevent detailing other aspects such as power system (Fazelpour et al. 2013; Isaienko et al. 2020; Dantsker et al. 2020), motors and propellers (Anon EPI 2020; Serrano et al. 2021), and the use of propellers instead of deflectable control surfaces for attitude control, winds, radiation, and other constraints. The risk-reduction process has gone from conceptual design to wind tunnel (gauging wing/sheet positioning and measuring aerodynamic coefficients), ground and low-altitude glide, and powered tests for strength, stability of Mylar sheets and flying wings, and robustness to gusts and sunlight/weather exposure. Flight simulation with present vehicle designs is being used to demonstrate performance and identify

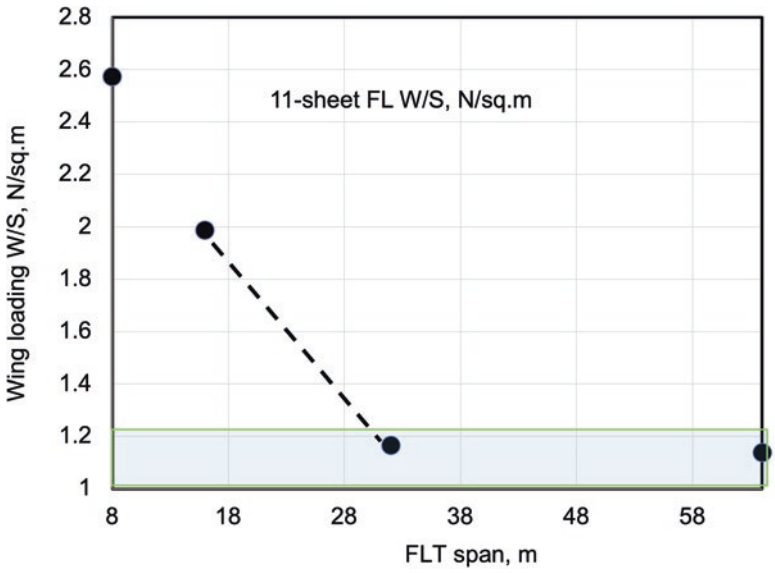

Fig. 16.5 A diagram showing why sheet spans of over 30 m are needed to achieve 12-h glide above 18.3 km

problems. Thermal and aeroelastic verification (Voß et al. 2020) and control strategies remain to be done.

16.3 Conclusions

Electric-aircraft aspects of Flying Leaflet (FLT) and Flying Leaf (FL) vehicles that comprise the initial Glitter Belt system are summarized in this short paper. The 30.5 km altitude and slow glide requirements provide unique challenges. Conceptual design, small scale design-build-fly tests, and dynamic flight simulation are used to remove uncertainties and derive properties of this system. The FLT, a 32 m-span, 4 m-chord, 4-propeller flying wing, carries a variably-deployed Mylar sheet to 30.5 km, and joins with 10 other similar craft to form an FL with 12 BLDC motors driving low-inertia propellers. The rise of solar power with altitude is a unique feature. Motor cooling in near-vacuum, rendezvous and swarm operation for high-precision distributed antenna applications pose unique challenges. Rendezvous and swarm operation for high-precision distributed antenna applications pose unique challenges and opportunities.

Acknowledgements This work was partially supported by the Taksha Institute.

References

D. Ackermann, A. Bierig, N. Reininghaus, *Modeling Spectrum Dependent Characteristics of Triple Junction Solar Cells for Solar-Powered Aircraft*, in 2021 Annual Modeling and Simulation Conference (ANNSIM) (IEEE, 2021, July), pp. 1–12

Anon EPI, Propeller Performance Factors. An Introduction to Propeller Technology. EPI Inc. Based on Aircraft Propeller Design, F. E. Weick, 1930 (2020, January 1), 452 p. Viewed 14/11/2021. http://www.epi-eng.com/propeller_technology/selecting_a_propeller.htm

O. Dantsker, M. Caccamo, S. Imtiaz, *Propulsion System Design, Optimization, Simulation, and Testing for a Long-Endurance Solar-Powered Unmanned Aircraft*, in AIAA Propulsion and Energy 2020 Forum (2020), p. 3966

F. Fazelpour, M. Vafaeipour, O. Rahbari, R. Shirmohammadi, Considerable parameters of using PV cells for solar-powered aircrafts. Renew. Sust. Energ. Rev. **22**(2013), 81–91 (2013)

L. Gilbert, Sail section lift, in *Technical & Theoretical Aspects of RC yacht racing. Lester Gilbert's Radio Sailing*. November 2020. http://www.onemetre.net/design/sailsect/sailsect.htm

V. Isaienko, V. Kharchenko, M. Matiychyk, I. Lukmanova, *Analysis of Layout and Justification of Design Parameters of a Demonstration Aircraft Based on Solar Cells*, in E3S Web of Conferences, vol. 164 (EDP Sciences, 2020), p. 13007

N. Kleemann, S. Karpuk, A. Elham, *Conceptual Design and Optimization of a Solar-Electric Blended Wing Body Aircraft for General Aviation*, in AIAA Scitech 2020 Forum (2020), p. 0008

N. Komerath, S. Hariharan, D. Shukla, S. Patel, V. Rajendran, E. Hale, *The Flying Carpet: Aerodynamic High-Altitude Solar Reflector Design Study (No. 2017-01-2026)*. SAE Technical Paper (2017)

N. Komerath, A. Sharma, R. Deepak, A. Deepak, *Glitter Belt Global Measurement System: Indian Ocean Component Preparation*, in Proceedings of the IEEE ICECCME 2021, Mauritius (October 2021a)

N. Komerath, R. Deekak, A. Deepak, *Flight Testing and Simulation of High Altitude Reflector Components*, in Proceedings of ISSA2021, Bangkok, Thailand (November 2021b)

J.R. Quinlan, *System and Method for Modular Unmanned Aerial System*. US Patent 10,196,143 B2 (5 Feb 2019)

Y. Ravikovich, L. Ponyaev, M. Kuprikov, R. Domjan, *Innovation Design Analysis of the Optimal Aerodynamic Adaptive Smart Structures for Disk-Body Solar Hybrid Electric Aircraft and Airship Concept*s, in IOP Conference Series: Materials Science and Engineering, vol. 1024, no. 1 (IOP Publishing, 2021), p. 012078

J.R. Serrano, A.O. Tiseira, L.M. García-Cuevas, P. Varela, Computational study of the propeller position effects in wing-mounted, distributed electric propulsion with boundary layer ingestion in a 25 kg remotely piloted aircraft. Drones **5**(3), 56 (2021)

V. Smil, *Energy Conversion Efficiency is Falling*. IEEE Spectrum February, 18–19. PDF (2021)

A. Voß, V. Handojo, C. Weiser, S. Niemann, Preparation of Loads and Aeroelastic Analyses of a High Altitude, Long Endurance, Solar Electric Aircraft (2020)

M. Wu, Z. Shi, T. Xiao, H. Ang, Effect of wingtip connection on the energy and flight endurance performance of solar aircraft. Aerosp. Sci. Technol. **108**, 106404 (2021)